LA-UR- 08-7791

Approved for public release; distribution is unlimited.

Title:	Anomalous yield reduction in direct-drive DT implosions due to 3He addition
Author(s):	H.W. Herrmann, J.R. Langenbrunner, J.M. Mack, J.H. Cooley, D.C. Wilson, S.C._Evans, T.J. Sedillo, G.A. Kyrala, S.E. Caldwell, C.S. Young, A. Nobile, J. Wermer, S. Paglieri, A.M. McEvoy, Y.H. Kim, S.H. Batha, LANL; C.J. Horsfield, D. Drew, W. Garbett, M. Rubery, AWE, V. Yu. Glebov, S. Roberts, LLE; J.A. Frenje, MIT
Intended for:	Special Issue of Physics of Plasmas covering the 50th Annual Meeting of the Division of Plasma Physics The American Physical Society November 17-21, 2008, Dallas, Texas

Los Alamos
NATIONAL LABORATORY
EST. 1943

Form 836 (7/06)

Anomalous yield reduction in direct-drive DT implosions due to ^{3}He addition

H.W. Herrmann, J.R. Langenbrunner, J.M. Mack, J.H. Cooley, D.C. Wilson, S.C. Evans, T.J. Sedillo, G.A. Kyrala, S.E. Caldwell, C.S. Young,
A. Nobile, J. Wermer, S. Paglieri, A.M. McEvoy, Y. Kim, and S.H. Batha
Los Alamos National Laboratory, Los Alamos, NM 87545

C.J. Horsfield, D. Drew, W. Garbett, and M. Rubery
Atomic Weapons Establishment, Aldermaston, U.K.

V. Yu. Glebov and S. Roberts
Laboratory for Laser Energetics, University of Rochester, Rochester, New York 14623

J.A. Frenje
Plasma Science and Fusion Center, Massachusetts Institute of Technology, Cambridge, Massachusetts 02139

Abstract:

Glass capsules were imploded in direct drive on the OMEGA laser [T. R. Boehly *et al.*, Opt. Commun. **133**, 495, 1997] to look for anomalous degradation in DT yield (i.e., beyond what is predicted) and changes in reaction history with ^{3}He addition. Such anomalies have previously been reported for D/^{3}He plasmas, but had not yet been investigated for DT/^{3}He. Anomalies such as these provide fertile ground for furthering our physics understanding of ICF implosions and capsule performance. A relatively short laser pulse (600 ps) was used to provide some degree of temporal separation between shock and compression yield components for analysis. Anomalous degradation in the compression component of yield was observed, consistent with the "factor of two" degradation previously reported by MIT at a 50% ^{3}He atom fraction in D_2 using plastic capsules [Rygg et al., Phys. Plasmas 13, 052702 (2006)]. However, clean calculations (i.e., no fuel-shell mixing) predict the shock component of yield quite well, contrary to the result reported by MIT, but consistent with LANL results in D_2/^{3}He [Wilson, *et al.*, Jrnl Phys: Conf Series 112, 022015 (2008)]. X-ray imaging suggests less-than-predicted compression of capsules containing ^{3}He. Leading candidate explanations are poorly understood Equation-of-State (EOS) for gas mixtures, and unanticipated particle pressure variation with increasing ^{3}He addition.

I. Introduction

Inertial Confinement Fusion (ICF) implosions have been conducted at U.S. laser facilities such as NOVA, OMEGA and soon at the nearly completed National Ignition Facility (NIF). OMEGA experiments are based predominantly on direct drive, in which laser beams impinge directly on the ICF capsule. NOVA was, as NIF will be, based predominantly on indirect drive in which the laser beams impinge upon the inside of a hohlraum, generating a uniform bath of x-rays which indirectly illuminate the capsule. In both cases, ablation of outer capsule material results in a rocket effect which compresses the remaining capsule material inward.

Fusion product yield can be separated into 2 components- shock and compression yield. If the velocity of the laser-driven shock is greater than the maximum velocity of the shell, the shock can break out of the shell, travel inward through the fusion fuel, rebound at the center of the capsule and travel outward through the fuel again. As it does so, the fuel ionizes and heats to high ion temperatures (e.g., ~10 keV), producing fusion yield before the capsule has reached maximum compression. The fuel can then cool back down after shock heating as the capsule continues to compress to maximum density, producing additional fusion yield at higher ion density but at lower ion temperature (e.g., ~5 keV). Ideally, shock and compression yields coincide, providing a synergy that maximizes fusion yield. However, experiments in which the final shell velocity is reduced, by using thick-walled capsules or by shortening of the laser pulse duration, enables one to study the individual yield components. Such studies allow additional insights into the dynamics of capsule implosions. Discerning these components of yield necessitates the ability to measure DT reaction histories with high precision. This study used the Gas Cherenkov

Detector (GCD) [Refs], developed at Los Alamos National Laboratory, which relies on the DT fusion gamma-ray output for high-bandwidth measurements (~4 GHz). Gaussian decomposition of the reaction history allows one to approximate the separate bang times (i.e., time of peak of fusion reactivity) and total yields for each yield component.

While relatively efficient in terms of laser energy coupling, direct drive can also result in a higher level of spatial non-uniformities giving rise to hydrodynamic instabilities, such as the Rayleigh-Taylor instability. These instabilities are known to result in fuel/shell mix which acts to cool the fuel and degrade the fusion yield. Radiation hydrodynamics codes (1-D and 2-D) are routinely used to calculate the performance of these implosions. These codes, however, typically over-predict the neutron yield, generally by factors of 2 to 4. Fuel-shell mix is often invoked in order to degrade the "clean" yield calculation and match the experimentally measured values.

In the current study, ^{3}He was added to capsules containing deuterium and tritium fuel. The ^{3}He was observed to degrade the fusion yield more than predicted by 1-D rad-hydro calculations. Yield degradation was predominantly found to occur in the compression component, with no significant effect on the shock yield. Increased mix as a result of ^{3}He addition does not provide a reasonable explanation. Instead, observations appear consistent with reduced compressibility, relative to calculations, of the capsule with ^{3}He addition. Several potential mechanisms are being explored to explain this reduced compressibility.

The paper is organized as follows: Previous work and motivations for the current study are presented in Section II, the experimental setup is presented in Section III,

experimental observations in Section IV, a discussion covering reduced compressibility and fuel/shell mixing are in Section V, and conclusions are presented in Section VI.

II. Motivation for ^{3}He in DT

The use of surrogate fuels provides a means of characterizing capsule performance without incurring the complications associated with the high fusion output of DT fuel. D_2 has been the most commonly used surrogate, but the primary interest is in DT since the first igniting capsules will surely contain pure DT. When an unexplained anomaly is discovered using a surrogate, it is not obvious whether this anomaly will also exist for DT and thus must be verified. The incorporation of ^{3}He appears to provide such an anomaly. Once understood, this anomaly could potentially lead to new physics insights and might even prompt the intentional addition of ^{3}He to DT as a diagnostic tool.

While the use of DT may complicate some diagnostic methods, it also enables the use of other valuable techniques. The high fusion output coupled with a relatively high fusion gamma-to-neutron branching ratio for the DT reaction enables the measurement of the 16.75 MeV gamma-rays that are emitted in just a few of every 100,000 DT fusion reactions. The time-resolved Gas Cherenkov Detector (GCD) [GCD Refs] was used in these studies for measurement of quality reaction histories based on the DT gamma-ray.

Previous ICF implosions have revealed the possible anomalous effect on fusion yield arising from mixtures of D_2 and ^{3}He. The most notable is a study lead by a team of MIT researchers in which a series of plastic capsules containing "hydro-equivalent" mixtures of D_2/^{3}He were imploded at the OMEGA laser [Rygg]. They discovered the compression and shock yield components were degraded relative to predictions scaled from pure D_2, with the maximum deviation occurring at 50% ^{3}He by atom.

Hydrodynamic-equivalency was satisfied in this previous study by maintaining a constant Atwood number. This is achievable since D and ^{3}He have the same value of (1+Z)/A, where Z is the atomic number and A the atomic mass. Mixtures can then be chosen such that the mass density and total particle density (ions + electrons) are identical. This is accomplished by exchanging three D-atoms for two ^{3}He-atoms. Once the fuel is fully dissociated and ionized after the first passage of the laser driven shock, the fuel is predicted to behave as an ideal gas (pV=nRT). Assuming the different fuel gas mixtures achieve the same temperature profiles upon ionization, the compression and degree of shell/fuel mix for these mixtures should be nearly identical and the fusion yield should closely follow a simple scaling based on the fuel composition ratios. However, the MIT group observed that the scaled DD neutron and D/^{3}He proton yields, normalized to pure D_2, were lower than predicted by a factor of ~2 in mixtures containing 50:50 D/^{3}He by atom. These trends were observed for both shock and compression yield components. Measurements of the areal density (ρR) suggested that gas mixtures experience less compression than purer D_2 or ^{3}He target fills do, in contradiction to the hydro-equivalent design hypothesis. Less compression alone however, wasn't sufficient to explain the magnitude of the yield discrepancy. In addition, no single physical mechanism has been identified to explain the observations, particularly the non-monotonic dependence on ^{3}He fraction. Comparisons of the current effort to this study will be presented in Section V.A).

A similar abnormal effect from ^{3}He has been identified in glass capsule implosions during "Hi-Z" experimental campaign at OMEGA being conducted by Los Alamos National Laboratory [Wilson]. These experiments were also designed to be hydro-equivalent. In this study, properly hydro-scaled burn histories without and with ^{3}He (20%

by atom) agree well until the time that the rebounding shock strikes the incoming shell, after which there is a divergence with less scaled yield coming from the capsule containing ^{3}He. Since the majority of shock yield occurs during the earlier period, the MIT conclusion that shock yield is anomalously affected by ^{3}He fraction is not supported. Degradation of compression yield however, appears to be consistent with that observed by the MIT group.

Implosions devised to be hydrodynamically equivalent, are all expected to exhibit the same radius versus time, independent of ^{3}He fraction. Contrary to this expectation, differences in shell radius with and without ^{3}He were observed from gated X-ray images. Shell X-ray emission suddenly brightens when the rebounding shock strikes the incoming shell. At this time, the X-ray image radius for the case with and without ^{3}He are in agreement and are consistent with simulation. After this time, however, the case with ^{3}He diverges, resulting in a ~25% larger radius at bang time than the case without ^{3}He and from the simulation.

III. Experimental Setup

Spherical SiO_x shells were fabricated by General Atomics using the glow discharge plasma (GDP) method [Hoppe]. The capsules had a mean diameter of 1098 ± 5 μm and a 4.7 ± 0.05 μm average wall thickness. All capsules were filled with 5.1 atmospheres of 50:50 DT gas at room temperature. Residual gases, predominantly CO_2 and CO, were estimated to be <0.13 atmospheres. ^{3}He was added after the DT fill, increasing the overall pressure. Three ^{3}He partial pressures were chosen, producing capsules that were not hydrodynamically equivalent to one another, and thus shot-to-calculation

comparisons were required for analysis. Future experiments will strive to obtain hydro-equivalency, making analysis of shot-to-shot comparisons more direct.

Accurate knowledge of the ^{3}He partial pressure in the capsule at shot time is critical for measuring ^{3}He effects on ICF implosions. Helium, being a small atom, naturally has a much higher permeation rate than hydrogenic molecules such as D_2, DT, and T_2. Typical room-temperature permeation half lives for DT through thin glass shells are on the order of 10 weeks, whereas the half life for ^{3}He is only a few hours. To minimize uncertainty, ^{3}He permeation rates for each individual capsule were measured by a pressure increase method [Wermer] after the shells had already been filled with 5.1 atmospheres of 50:50 DT gas. The results, shown in Figure 1, indicate a mean ^{3}He permeation half life of 2.5 hours. All permeation rates were within ± 0.5 hour of this mean. Capsules were stored in individual ^{3}He-pressurized containers to prevent leakage.

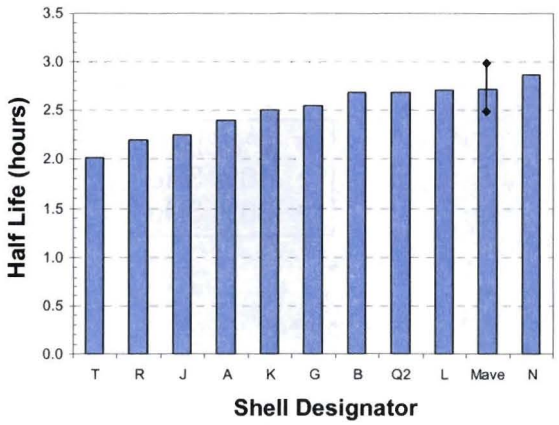

Figure 1: ^{3}He permeation half lives for each individual SiO_x shell used on shot day. Error bars on shell M show reproducibility of measurement.

Shells were kept on dry ice to minimize leakage of DT, with the exception of short periods to conduct the ^{3}He permeation tests, to mount and place them in the ^{3}He-pressurized cells, and before target chamber insertion on shot day. Time at room

temperature was carefully recorded to produce an accurate estimate of DT partial pressure at shot time. The time between taking a target from a ^{3}He-pressurized cell and shot time was also recorded. To minimize ^{3}He leakage and the uncertainty in the ^{3}He partial pressure at shot time, this delay was kept as short as practical. Figure 2 shows the estimated ^{3}He concentration as a function of the time-to-shot for the three separate fill pressures. The delay between taking a target out of a ^{3}He-pressurized cell and shot time was limited to less than 35 minutes for all shots, with all but one shot occurring within 25 minutes. As a result, uncertainty in the ^{3}He concentration was better than ±3%. It is estimated that the targets that were not intentionally filled with ^{3}He had no more than 12 ppm ^{3}He resulting from equilibrium between continuous source (tritium decay) and loss terms (permeation).

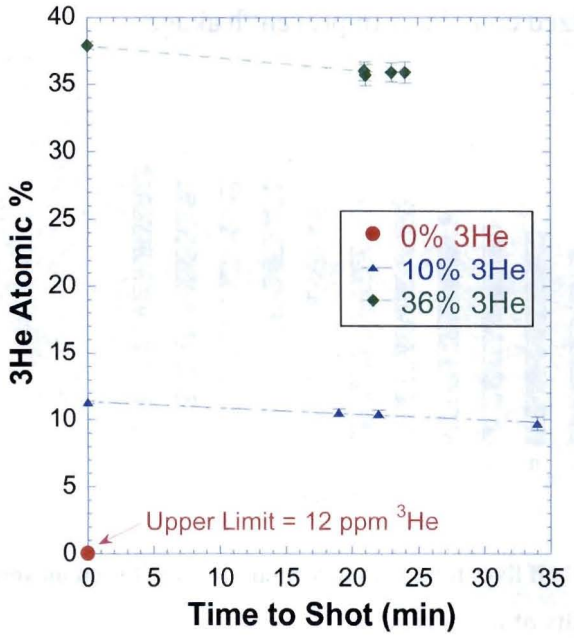

Figure 2: Estimated ^{3}He concentration at shot time based on individual leak rates of Figure 1. Capsules contained ~5 atm of DT at shot time. Capsules were stored for several days in cells pressurized with ^{3}He to either 0, 1.26 or 6.05 atm, resulting in ^{3}He atomic concentrations at shot time averaging 0, 10 or 36%, respectively. Data points on the y-axis represent the ^{3}He concentration just before depressurization of the gas cell and are for illustrative purposes only.

Direct-drive implosions of these targets were conducted at OMEGA using 60 beams of frequency-tripled (351 nm) UV light in a 0.6 ns square pulse and a total energy of 16.4 kJ with no smoothing by spectral dispersion (SSD). This relatively short laser pulse (as compared to the more typical 1 ns pulse used in the other previously cited studies) was chosen to reduce and delay the compression component of the yield so that the shock component would be more discernable in neutron and gamma-based reaction history measurements. As-shot conditions are summarized in Table 1.

	SiGDP Shell		DT Fill Pressure at Shot Time	3He Pressure at Shot	Total Pressure at Shot Time	3He Fraction	Laser Energy	nTOF Ti	nTOF neutron Yield	Yield Over Clean
Shot #	ID (um)	Wall (um)	(atm)	(atm)	(atm)	(Atomic %)	(kJ)	(keV)	(1e12)	
47875	1097	4.6	5.00	0.00	5.00	0.0%	16.0	4.81	8.8	0.37
47877	1094	4.7	5.00	0.00	5.00	0.0%	16.3	5.06	9.11	0.38
47881	1097	4.7	4.99	0.00	4.99	0.0%	16.5	5.3	8.69	0.37
47879	1097	4.7	4.97	1.07	6.04	9.7%	16.3	4.69	5.12	0.41
47873	1112	4.7	4.87	1.14	6.01	10.4%	16.3	4.83	4.77	0.38
47876	1100	4.6	4.93	1.16	6.09	10.5%	16.0	4.64	4.19	0.33
47880	1098	4.6	4.97	5.51	10.48	35.7%	16.4	4.94	1.69	0.39
47874	1098	4.7	4.94	5.53	10.47	35.9%	16.4	4.55	1.7	0.40
47878	1093	4.6	4.96	5.57	10.53	35.9%	16.4	5.15	1.5	0.35
47882	1096	4.6	4.95	5.58	10.52	36.0%	16.3	4.87	1.43	0.33
"0 atm" AVE	1096.0	4.67	5.00	0.00	5.00	0.0%	16.27	5.06	8.87	0.37
"1.1 atm" AVE	1103.0	4.67	4.92	1.12	6.05	10.2%	16.20	4.72	4.69	0.37
"5.6 atm" AVE	1096.3	4.63	4.95	5.55	10.50	35.9%	16.38	4.88	1.58	0.37
Overall AVE	**1098**	**4.7**	**5.0**				**16.3**	**4.9**	**4.7**	**0.37**

Table 1: As-shot conditions.

IV. Experimental Observations

The addition of ^{3}He decreases the neutron yield as shown in Figure 3. The yield was measured by the neutron time-of-flight detector (nTOF) installed at 12.4 m from the target [V.Yu. Glebov et al., RSI, V 75, p. 3559, (2004)]. Shot-to-shot reproducibility was better than ±10% about the mean. DT fusion neutron yield drops by 80% between 0 and 36% ^{3}He by atom. Also plotted is the independently-determined DT fusion gamma yield

as measured by the GCD which shows the same trend in neutron yield as a function of ^{3}He concentration. A DT gamma-to-neutron branching ratio of $2x10^{-5}$ can be inferred from these data; however, uncertainty in the GCD absolute calibration is no better than a factor of 3 at this time. Recent values for the DT branching ratio vary from $5x10^{-5}$ to $1.2x10^{-4}$ [Kammeraad et al., 1993; Morgan et al., 1986; Cecil et al., 1985; Balbes et al., 1994]. However, the measurements described in the literature are based on beam-target experiments with ion beam energies in excess of 100 keV, and so may not be appropriate for thermonuclear fusion at ion temperatures ~5 keV. A 1-D radiation hydrodynamic simulation, assuming no mix between the shell material and fuel during compression (i.e. clean calculation), shows the measured yield is 0.37 of calculated for all ^{3}He concentrations. This is reflected in the value of Yield-over-Clean (YOC) in Table 1. This constant scale factor may be somewhat coincidental however, as will be discussed in Section V.

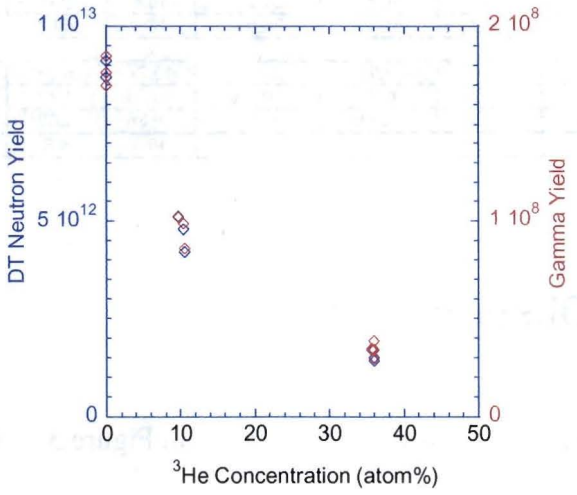

Figure 3: DT neutron and gamma yields as a function of ^{3}He concentration measured by nTOF (blue diamonds) and GCD (red diamonds), respectively.

Fusion reaction histories based on DT-gammas measured using the GCD and DT-neutrons measured using the Neutron Temporal Diagnostic (NTD) [Lerche] are shown in Figure 4. Since the relative time base of the GCD instrument is not absolutely calibrated, it is cross-calibrated against the absolutely calibrated NTD by matching bang-times on what was considered to be the shot with the best quality NTD data (shot 47877). The time base offset relative to an optical timing fiducial is determined from this "best-case". This offset was then applied to the GCD timing, also relative to the optical timing fiducial, for the remaining shots [Herrmann]. Post processing to remove instrument temporal response was performed on both reaction history diagnostics. The standard NTD algorithm described in [Lerche] was used to remove the 1.2 ns decay time of the NTD scintillator. Deconvolution is able to remove much of the GCD instrument impulse response time of approximately 135 ps fwhm, leaving a residual response of approximately 70 ps fwhm. The reaction histories for 0% ^{3}He show an asymmetry which evolves into an observable feature on the leading edge of the GCD signal at 10% ^{3}He addition, and finally becomes a discernibly separate peak at 36% ^{3}He.

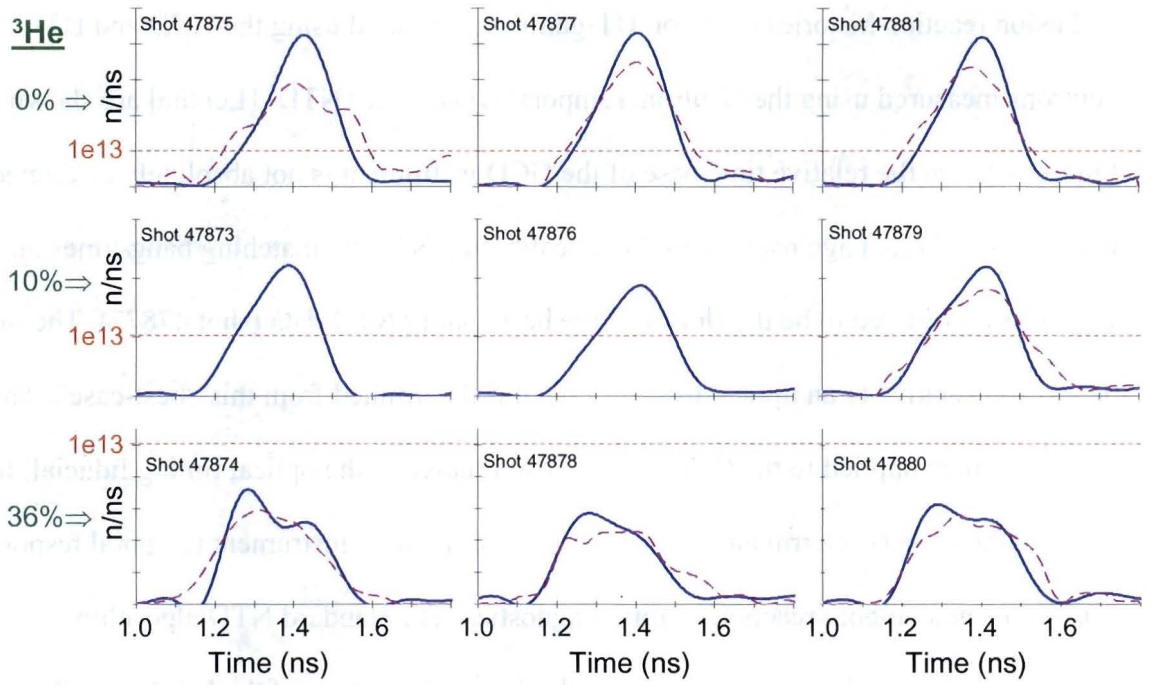

Figure 4: DT fusion reaction histories from the Gas Cherenkov Detector (solid blue line) and the Neutron Temporal Diagnostic (dashed pink line) show the growth of a feature near 1.25 ns as ^{3}He is added. Instrument response has been deconvolved from the data for both detectors. No NTD data was acquired on 2 shots (47873 & 47876). NTD data for Shot 47877 was used to establish an absolute time base for the GCD data.

Time-integrated ion temperature measurements using the neutron time-of-flight detector (nToF) are displayed in Figure 5. There does not appear to be a strong temperature dependence with ^{3}He concentration although calculations indicate a monotonic temperature decrease with increasing ^{3}He, whereas a slight increase was detected in going from 10 to 36% ^{3}He.

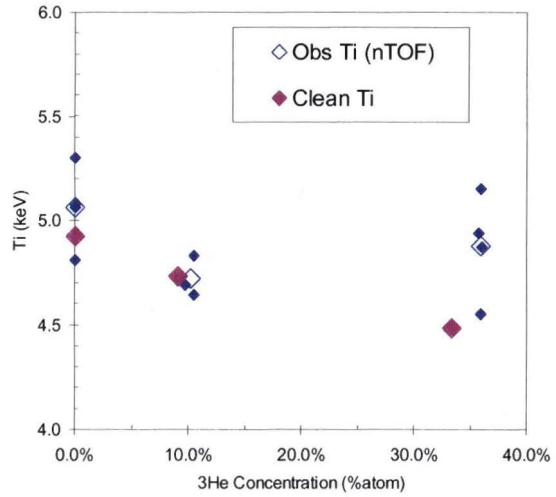

Figure 5: Burn averaged ion temperature measured by neutron Time-of-Flight (nTOF) in solid blue diamonds, the mean of the measurements in open blue diamonds, and a clean calculation (i.e., no shell/fuel mix) in solid pink diamonds.

The shell radius trajectory for one shot at 36% ^{3}He addition as inferred from gated X-ray images measured using the QXI diagnostic [Ref?] is shown in Figure 6. X-rays become observable once the shock wave rebounding from the center strikes the incoming shell, establishing a time reference for comparison with simulation. Also shown are the simulated x-ray image radii based on the clean calculation. From the reaction histories of Figure 4, we find that the bang time for the compression component of yield, occurs at about 1.44 ns. From Figure 6 it appears that the shell radius is about 25% larger than simulated by a clean calculation at this bang time, corresponding to approximately a factor of two larger volume.

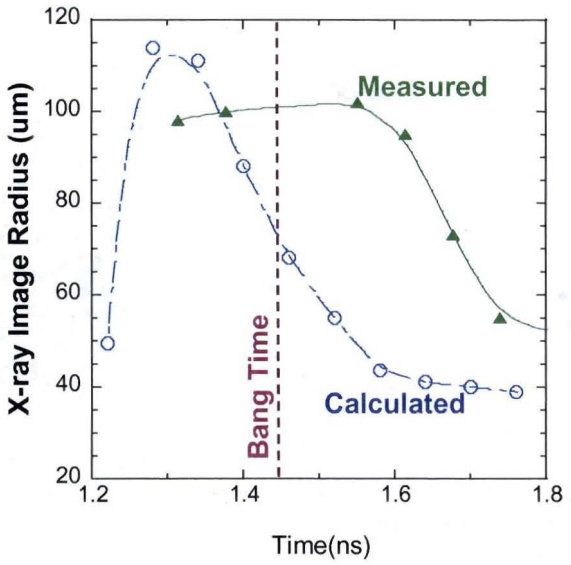

Figure 6: Temporal dependence of X-ray image radius for a 36% ^{3}He shot from the gated x-ray imager (QXI) green diamonds), and clean calculation (open blue circles) shows less compression than expected.

V. Discussion

Several possible physical mechanisms pertaining to differences in composition, temperature, density, burn volume, and burn duration of the target during the implosion were explored in [Rygg] in an attempt to explain the effect of mixtures containing ^{3}He. Some of them have the potential to explain reduced scaled yield in going from 0% ^{3}He to 50% ^{3}He, but none offer the possibility of explaining the recovery in scaled yield in going from 50% ^{3}He toward 100% ^{3}He. Although the current study has not yet explored the region from 50% to 100% ^{3}He, it is likely that this non-monotonic behavior also exists in DT/^{3}He implosions, and will be equally difficult to explain. Here we focus on the apparent symptoms of reduced compressibility and compression yield and their possible causes, and then examine and attempt to discount fuel/shell mixing as a possible cause of the reduced compression yield by itself.

A. Reduced Compressibility

Rather than simply investigate total yield degradation, it is more insightful to examine the shock and compression yield components individually as we explore mechanisms of yield degradation from the clean model. For this purpose, we decompose both the GCD-measured and the calculated reaction histories into two Gaussian components which are representative of the early shock yield and the later compression yield. The Gaussian decomposition for the GCD reaction histories are shown in Figure 7. These curves are a composite representing the 3 or 4 shots taken at each ^{3}He concentration. These composite GCD reaction histories are compared to the calculated reaction histories in Figure 8. It is evident that the observed compression yield degrades more quickly with increasing ^{3}He than is predicted by calculation.

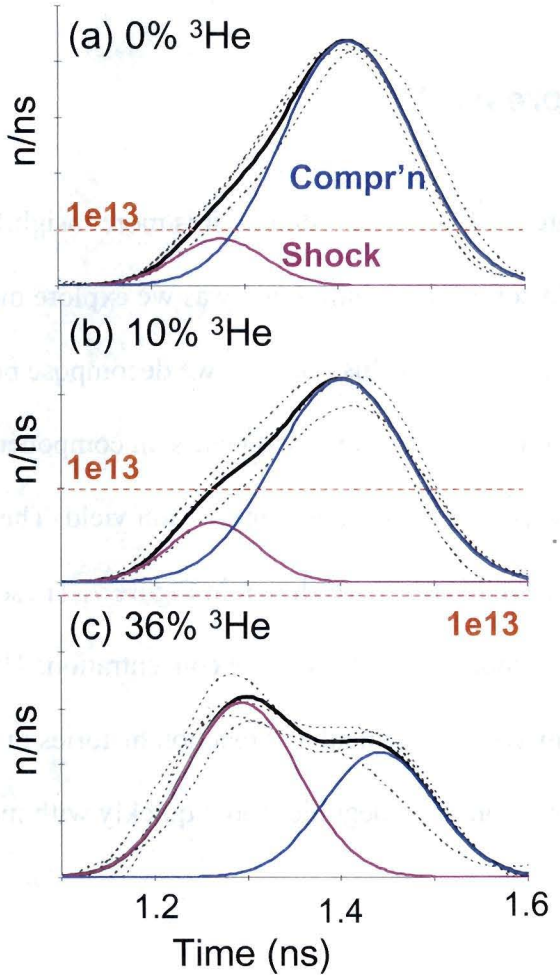

Figure 7: Gaussian decomposition of reaction histories measured using the GCD instrument for (a) 0% ^{3}He, (b) 10% ^{3}He, and (c) 36% ^{3}He addition. Individual deconvolved reaction histories at each ^{3}He concentration are shown in dashed lines. Composites of the Gaussian fits to each of these reaction histories are shown in solid lines for the yield components arising from Shock (pink) and Compression (blue), with their sum in bold black lines. Vertical scale is linear with the 1x10^{13} n/ns line shown in each case by a red dashed line for reference.

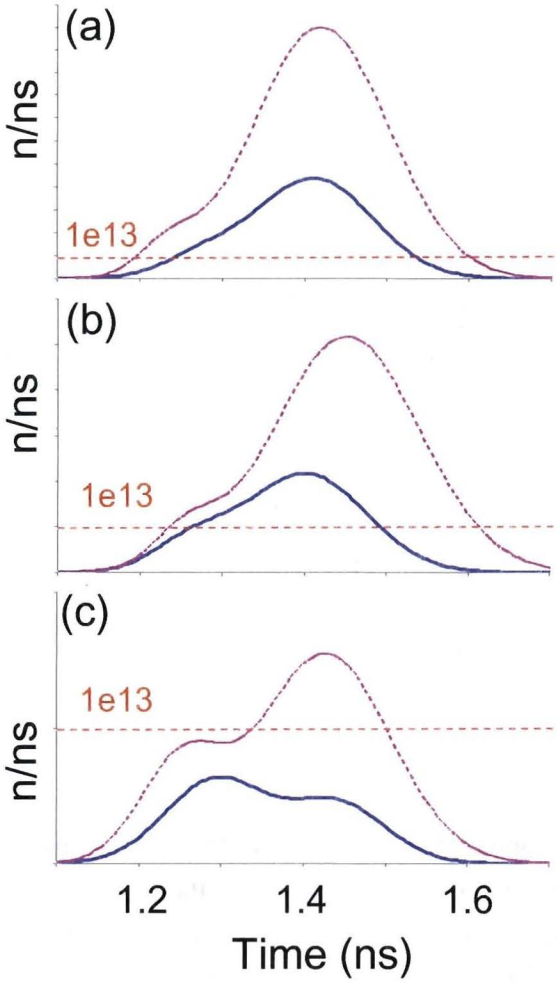

Figure 8: Comparison of the composites of measured reaction histories (blue solid line) and calculated (pink dashed line). Calculated histories are convolved with a 20 ps Gaussian to simulate instrument response.

The Gaussian fit parameters for the decomposed reaction histories of Figure 7 are presented in Figure 9. For the shock component of the yield, the clean calculation is reasonably consistent with the observations. These data are suggestive of a shock yield that burns at a higher rate (Figure 9 (a)) for a shorter period of time (Figure 9 (b)) than calculated, but this difference is within the uncertainties of the analysis. The resulting neutron yield (Figure 9 (d)) and bang time (Figure 9 (c)) for the shock component display good agreement between calculated and observed.

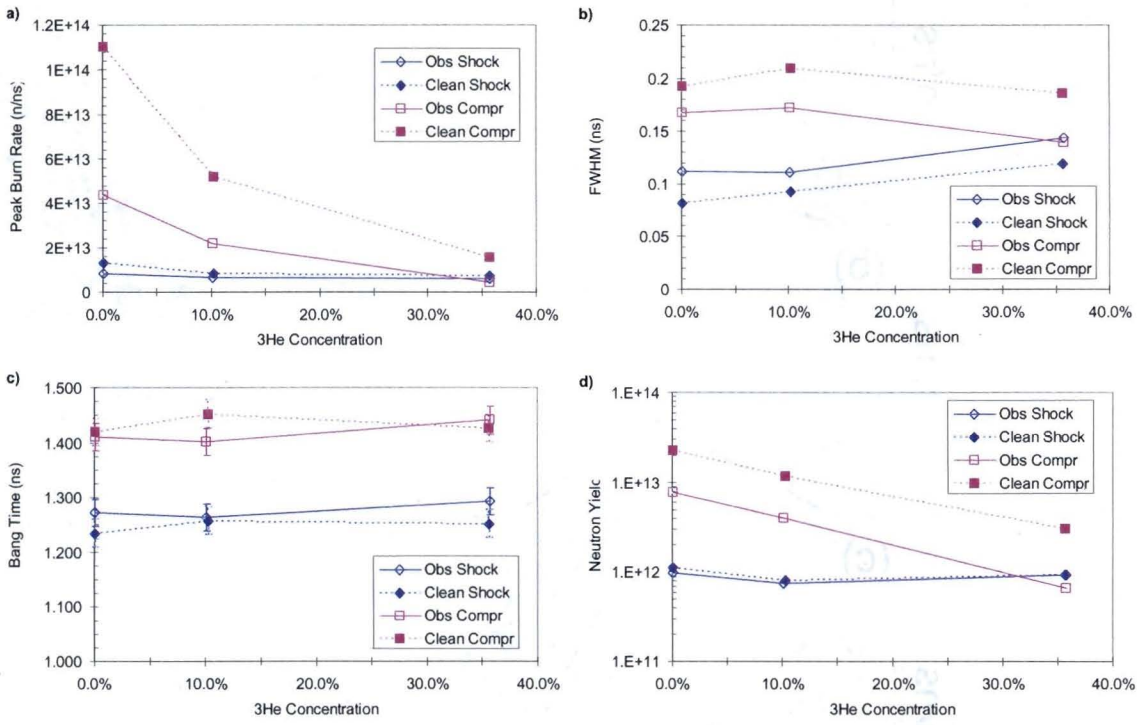

Figure 9: Reduction of Gaussian fits into a) Peak Burn Rate, b) Full width at half maximum (FWHM), c) Bang Time and d) Neutron Yield =1.06 x Peak Burn Rate x FWHM (semi-log scale). Parameters from the fit to experimentally measured reaction histories (after deconvolution) are shown in open symbols/solid lines (i.e. Obs), and those from the fit to calculated reaction histories assuming no mix are shown in solid symbols/dashed lines (i.e. Clean). Shock components are in blue diamonds and compression components are in pink squares.

The compression yield, however, shows a considerable discrepancy between calculated and observed, with the calculated peak burn rate, fwhm and resulting compression neutron yield being significantly higher than observed. Bang times are in reasonable agreement for compression components, as they were for the shock components.

The ratio of the observed yields to the clean calculated yields using the Gaussian fit parameters is shown in Figure 10. The ratio for shock yield ranges from 86% to 98%, indicating the relatively good ability to predict shock yield. The observed compression

yield is 34% of calculated at 0 and 10% ^{3}He, but drops to 21% of calculated yield at 36% ^{3}He. The total yield-over-clean (YOC) ranges from 36% to 39%, consistent with the 37% YOC scaling determined in Table 1. The small differences arise from slight imperfections in the Gaussian fits. The YOC remains relatively constant as the fixed shock yield makes up for the loss of compression yield with increasing ^{3}He, and thus appears to be somewhat coincidental.

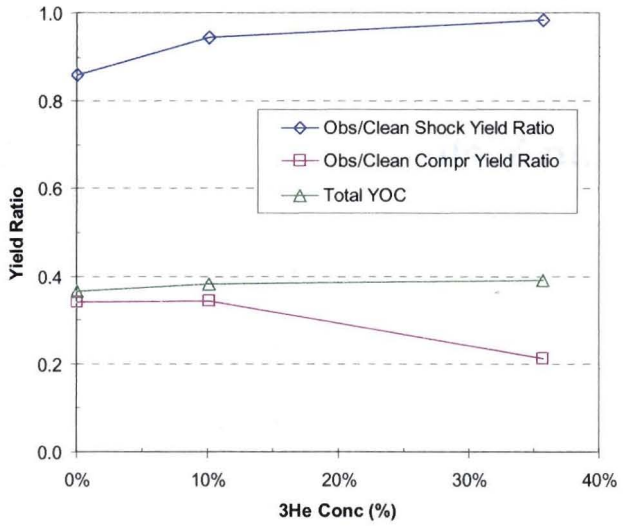

Figure 10: Ratio of Observed to Clean Calculated yields from Figure 10 d).

The observed YOC for the compression yield from Figure 10 is re-plotted in Figure 11 (a) after normalizing the data to one at 0% ^{3}He so that a direct comparison to the MIT results can be made. It can be seen that the anomalous compression yield degradation in DT/^{3}He-filled glass capsules is consistent with that previously seen in D_2/^{3}He-filled plastic capsules.

The YOC for the shock yield from Figure 10 is re-plotted in Figure 11 without normalization. For the shock yield we see reasonable agreement with calculation, whereas the MIT study observed a non-monotonic trend for the 24 μm thick capsules

very similar to what was observed for compression yield. For the 20 μm thick capsules, however, there does not appear to be a strong trend with ^{3}He. It should be noted however that the 20 μm shock yield data was considered to have too high a level of uncertainty from which to draw any conclusions, hence the lack of error bars. As previously mentioned, a Los Alamos study using $D_2/^3$He-filled glass capsules also observed YOC trends that were consistent with the MIT compression yield results, but did not see an anomalous effect in shock yield.

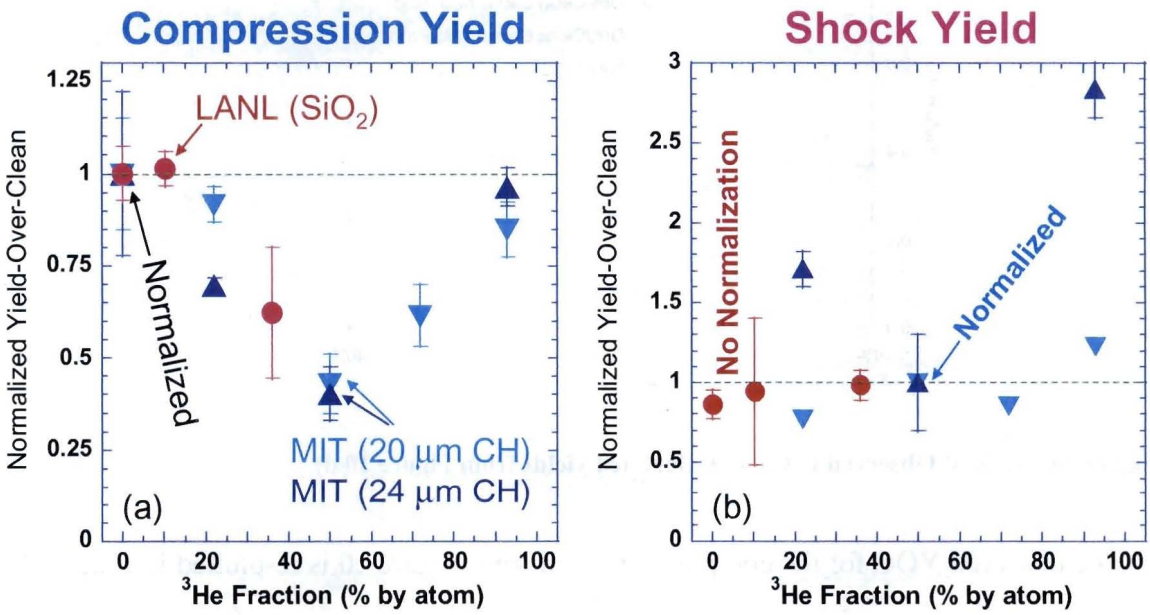

Figure 11: Yield over clean for (a) compression yield component normalized at 0% ^{3}He and (b) shock yield component normalized at 50% ^{3}He for the MIT study and no normalization for the current study. In both frames, the MIT $D_2/^3$He-filled plastic capsules are shown in light blue downward pointing triangles for 20 μm thick CH capsules, and dark blue upward pointing triangles for 24 μm thick CH capsules. The current study using DT/^{3}He-filled 4.7 μm thick glass capsules are shown as solid red circles.

The gated x-ray imaging measurements shown in Figure 6 are consistent with less compression than predicted for 36% ^{3}He addition. No useful x-ray imaging data were obtained for the other ^{3}He concentrations. A 25% larger outer shell radius corresponds to approximately a factor of 2 less fusion yield, assuming a fixed shell ρR and fuel ion temperature such that the fusion yield is roughly proportional to $n_D n_T V \sim 1/r^3$. However, less compression is likely to result in lower ion temperature, reducing the yield further.

The nToF measurements shown in Figure 5 are also consistent with reduced compression at 36% ^{3}He. The nToF ion temperature is a burn averaged measurement. It becomes skewed to higher temperature when the shock yield component becomes comparable to compression yield, owing to the higher ion temperatures that occur during shock yield. The ratio of compression to shock yield at 36% ^{3}He is about 3:1 in the calculation and 1:1 in the experiment, as can be seen in Figure 7 (d). Assuming the ion temperature is 6.5 keV during shock and 4 keV during compression, the burn averaged ion temperature for 36% ^{3}He should go from ~4.4 keV in the calculation to ~5.0 in the experiment, similar to the results of Figure 5. Thus, the unpredicted increase in T_i in going from 10 to 36% ^{3}He can be explained by the unpredicted decrease in compression yield.

The underlying assumption of previous experiments examining the effect of ^{3}He is that the capsules are truly hydrodynamically-equivalent. This is based on the knowledge that the ionized gas acts an ideal gas. However, the details of the original non-ionized molecular gas will determine the shock jump conditions and thus the initial conditions for the compression of the ideal gas. Additionally, the hydro-equivalency is based solely upon charged particle number density and mass density equivalency, but has a

discrepancy in the individual ion and electron number densities since He contributes more electrons than D. This discrepancy leads to a change in the way energy is distributed between the ions and electrons in the fuel, and thus potentially causes a deviation from true hydro-equivalency.

These arguments prompted exploration in a new direction. Perhaps differences in equation of state (EOS) between DT and mixtures containing ^{3}He may be responsible for the observed behavior. Typically, the radiation hydrodynamics codes use an EOS for deuterium and isotopically scale this EOS to tritium and ^{3}He. J.H. Cooley, et al., [ref APS bulletin] are finding that the use of a proper mixture of DT EOS and ^{3}He EOS has the effect of changing the initial conditions of the ionized fuel and as a result reducing the compressibility and compression yield with increased ^{3}He.

In addition, preheating of fuel is being questioned [Wilson, private]. If ^{3}He is substantially more heated by fast electrons than DT, then a higher temperature and pressure may result in less compressibility. However, initial studies indicate that a significant amount of preheat would be required to achieve the factor of 2 reduction in scaled yield. In addition, this mechanism is unlikely to explain the non-monotonic behavior.

B. Mix

As previously noted, the YOC for all three He concentrations was 0.37. An often-used method for degrading the clean yield is to apply fuel/shell mixing models [Wilson, PoP03; Christneson, PoP04]. It is unlikely that mix will result in less compressibility, but must be examined as a possible cause of reduced compression yield since we haven't

conclusively demonstrated that the capsules don't compress as much as predicted at 36% ^{3}He.

Employing the Scannapieco and Cheng dynamic mix model [ref], it is found that a value of 0.065 for the mix parameter (α) is required to reduce the total yield to match the experiment with no ^{3}He. This value of α is in reasonable agreement with past experiments and mix may very well be a reasonable means to explain the yield degradation at 0% ^{3}He. However, this same value of α does not explain the degradation when ^{3}He is added. It is found that a significantly larger alpha, or more mix, is needed for larger values of ^{3}He concentration. The value of α must increase to 0.09 at 10% ^{3}He and 0.15 at 36% ^{3}He. Since additional ^{3}He also means additional pressure in the capsule (more than double in going from 0 to 36% ^{3}He) and therefore increased resistance to hydrodynamic instabilities, it is expected that the required alpha would decrease with increasing ^{3}He, not increase. Such pressure stabilization has been observed previously [Wilson]. In addition, mix is expected to produce an increasing degradation in burn/rate as the mixed material propagates toward the core. This should modify the reaction history by truncating the burn is such a way that the bang time for the compression component occurs earlier and the fwhm is reduced. The observed compression bang times shown in Figure 7 are relatively independent of ^{3}He concentration, and the reduction in fwhm is only about half of what would be expected with the level of required mix. Thus, it appears unlikely that increased fuel/shell mix with increasing ^{3}He is a viable explanation for the observed behavior.

VI. Conclusions

The anomalous degradation in measured yield previously observed in $D_2/^3He$-filled plastic and glass capsules has now been observed in $DT/^3He$-filled glass capsules in direct-drive ICF implosions. However, unlike the MIT results for $D_2/^3He$-filled plastic capsules, the anomaly appears to primarily affect the compression component of yield, and not the shock component. These observations are consistent with the results of a previous Los Alamos study using $D_2/^3He$-filled glass capsules. The results are not explained by increased fuel/shell mix with increasing ^3He. Diagnostic signatures are consistent with reduced capsule compressibility with increasing ^3He addition. These include: lower compression yield as determined by reaction histories measured using the Gas Cherenkov Detector and Neutron Temporal Diagnostic; larger shell radius as measured by gated X-ray imaging; and larger ion temperature as measured by Neutron Time of Flight (nToF). Several hypotheses have been advanced, but not conclusively proven.

Two future experiments can provide additional information to test these hypotheses. First, hydrodynamically-equivalent $DT/^3He$ gas mixtures will allow better shot-to-shot comparisons with less reliance on shot-to-calculation comparison[1]. Second, ^3He fractions greater $\geq 50\%$ would verify the non-monotonic behavior previously observed in $D_2/^3He$ implosions.

Acknowledgements:

Work supported by US DOE/NNSA, performed by LANL, operated by LANS LLC under Contract DE-AC52-06NA25396.

References:

[1] Preliminary hydro-equivalent DT/^{3}He capsule experiments appear to be consistent with reduced capsule compressibility. These experiments will be reported on separately once more data is gathered.